Chandra Observations of the Diffuse X-ray Emission in Pictor A Radio Galaxy

Rameshan Thimmappa[1], **Ł. Stawarz,**[1] **M. Ostrowski, A. Goyal,**

[1]Astronomical Observatory, Jagiellonian University, 30-244 Krakow, Poland

email : rameshan@oa.uj.edu.pl

Abstract

Here we present some preliminary results of our analysis of the *Chandra* observations of the diffuse X-ray emission from the extended lobes in Pictor A radio galaxy. All the available *Chandra* data for the target, consisting of multiple pointings spanning over 15 years and amounting to the total exposure time of 464 ks, have been included in the analysis. All the point and compact sources in the field – both unrelated background/foreground objects, as well as the unresolved core, the jet, and the hotspot regions of Pictor A – were removed, and the radio contours were superimposed on the *Chandra* image to define the edges of the lobes. This will allow us to calculate the ratio of the X-ray to radio (both total and polarised) fluxes of the non-thermal diffuse emission, as a function of the position within the lobes. Our main goal is an in-depth statistical analysis of the resulting distribution, offering a unique insight into the lobes magnetic field structure.

Chandra data and data analysis

Radio lobes of Pictor A, one of the most prominent radio galaxy in the sky, are characterized by the total angular extension of ~ 8 arcmin (Perley et al. 1997). The non-thermal X-ray emission of the lobes have been also detected with the *Chandra* X-ray Observatory (e.g., Hardcastle et al. 2016). As such, the source is the best target for a detailed investigation of the X-ray and radio flux distribution within the lobes, utilizing the matching arcsec resolution of *Chandra* and VLA. This analysis may, in principle, unveil the underlying distribution of relativistic electrons and magnetic field. Note that the observed synchrotron radio flux scales with the product of the magnetic field energy density, u_B, and the electron energy density u_e, namely $S_r \propto u_B \times u_e$, while the non-thermal X-ray flux, believed to be dominated by the inverse-Comptonization of the CMB radiation, scales as $S_x \propto u_e \times u_{cmb}$, where u_{cmb} is the energy density of the CMB photons. Hence, only the combined VLA and *Chandra* data analysis for Pictor A, may allow us to map independently the spatial distribution of u_e and u_B within the lobes.

However, the *Chandra* data analysis for the diffuse lobes in Pictor A is complicated by the fact that multiple *Chandra* pointings carried out over the last 15 years have been performed with different ACIS configurations, often not covering the entire source (see the Table below). As a result, the exposure across the lobes, as well as the *Chandra* point spread function (PSF), are highly non-uniform. In addition, due to the large angular extension of the target, there are numerous unrelated foreground and background X-ray sources. Finally, the bright core, the jet, and the hotspots regions, all contribute significantly to the total X-ray output of the source, contaminating the diffuse emission of the lobes.

OBsId	Obs date	Exp (ks)	DETNAME	SIM_Z	FP (K)	Sepn (′)	PA
346	2000-01-18	25.8	ACIS-23678	-190.143	164.0	0.7	+90
3090	2002-09-17	46.4	ACIS-235678	-190.143	153.4	2.7	-81
4369	2002-09-22	49.1	ACIS-235678	-190.140	153.4	2.7	-81
12039	2009-12-07	23.7	ACIS-235678	-190.140	153.4	0.6	+87
12040	2009-12-09	17.3	ACIS-235678	-190.140	153.4	0.6	+87
11586	2009-12-12	14.3	ACIS-235678	-190.140	153.4	0.6	+87
14357	2012-06-17	49.3	ACIS-235678	-190.140	153.4	0.4	+142
14221	2012-11-06	37.5	ACIS-235678	-190.140	153.6	0.3	+83
15580	2012-11-08	10.5	ACIS-235678	-190.143	153.4	0.3	+83
15593	2013-08-23	49.3	ACIS-235678	-190.143	153.4	0.2	+123
14222	2014-01-17	45.4	ACIS-235678	-190.140	153.9	0.5	+99
14223	2014-04-21	50.1	ACIS-235678	-190.143	153.4	0.5	+128
16478	2015-01-09	2 6.8	ACIS-235678	-190.140	153.8	0.5	+101
17574	2015-01-10	18.6	ACIS-235678	-190.140	156.7	0.5	+101

Merged exposure-corrected X-ray image

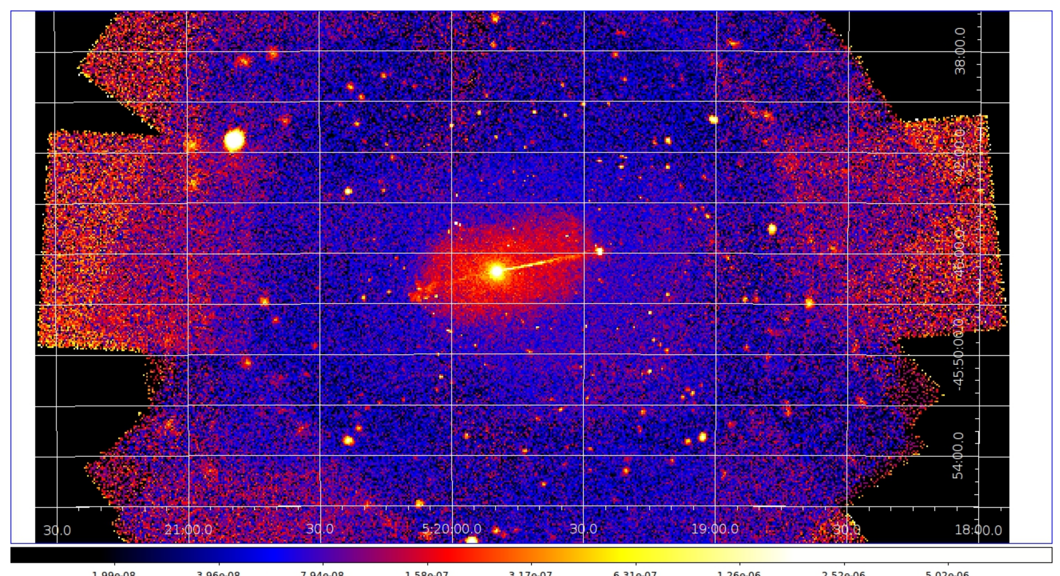

Figure 1: Merged and exposure-corrected *Chandra* image of Pictor A field, in the energy range 0.5–7.0 keV. The image shows the bright core of the radio galaxy in the center, the jet extending to the north-west from the core, the western hotspot, the eastern hotspot region, and the surrounding diffuse lobes.

Point and compact sources

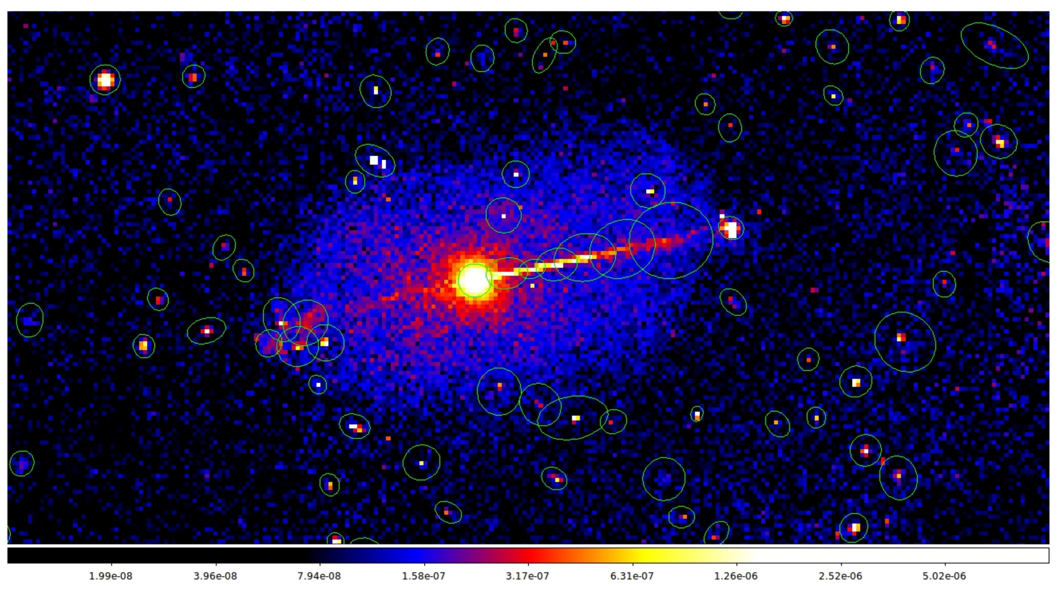

Figure 2: Point and compact sources (denoted by green regions) detected with the WAVDETECT tool using the "minimum PSF" method on the merged and exposure-corrected *Chandra* image of Pictor A. Different region sizes across the field reflect varying PSF and/or sources' extension.

Point and compact sources removed

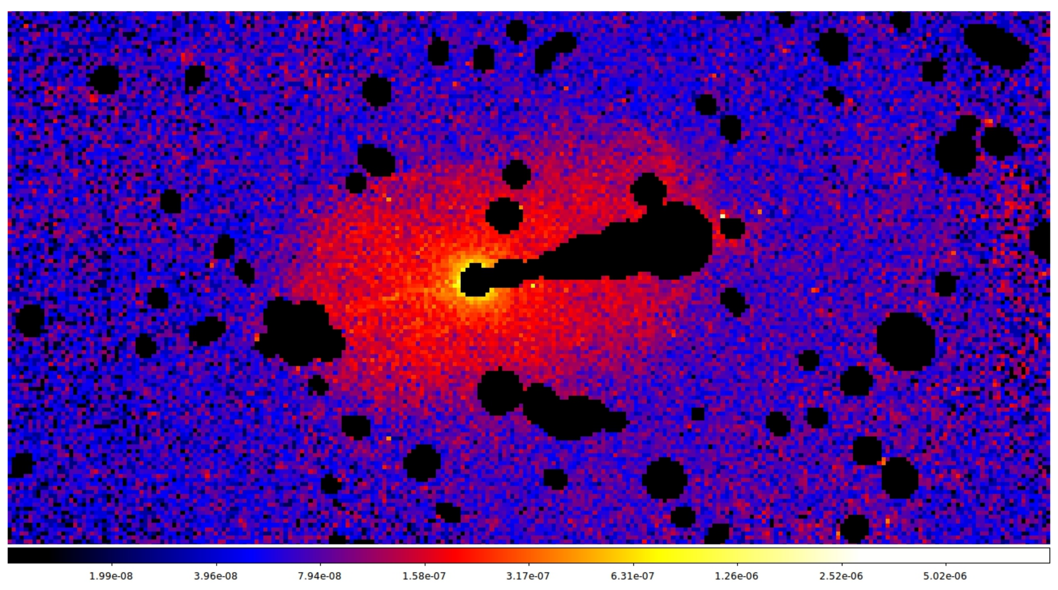

Figure 3: Merged and exposure-corrected *Chandra* image of Pictor A field, with all the point and compact sources removed, including the core, the jet, and the hotspots (note that these are different than the "exclusion regions" in the Pictor A lobes analysis by Hardcastle et al. 2016; also, no counter-jet feature has been removed).

X-ray vs. radio morphology

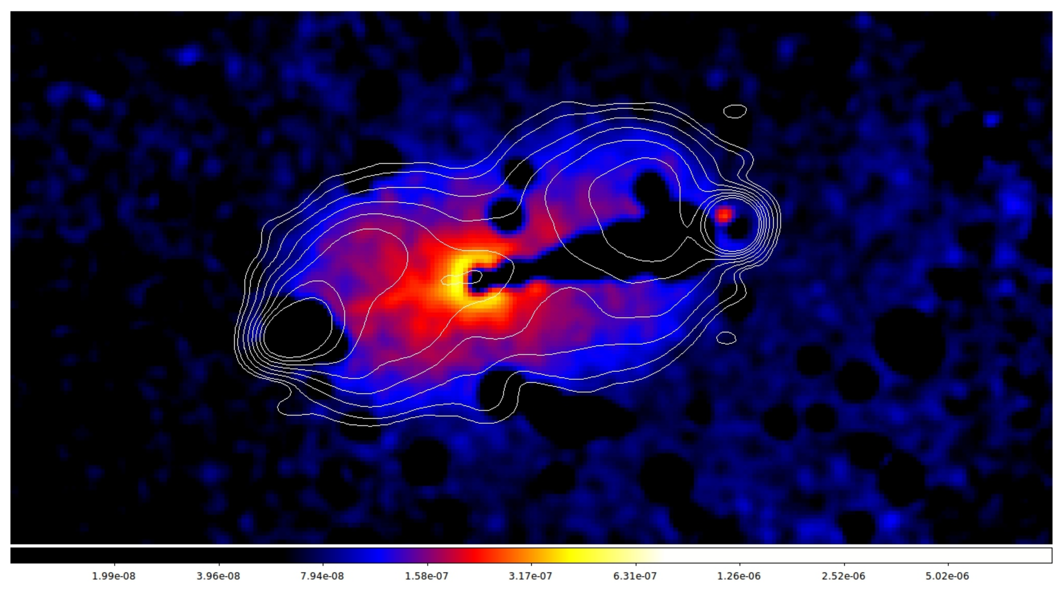

Figure 4: Merged and exposure-corrected smoothed *Chandra* image of the extended lobes in Pictor A in the energy range 0.5–7.0 keV, with the $\lambda 90$ cm radio contours superimposed. The radio contours with the intensity ratio $\sqrt{2}$ and $30''$ resolution are between 0.4% and 20% of the peak intensity of 23 Jy/beam (Perley et al. 1997).

Chandra + VLA $\lambda 20$ cm total intensity

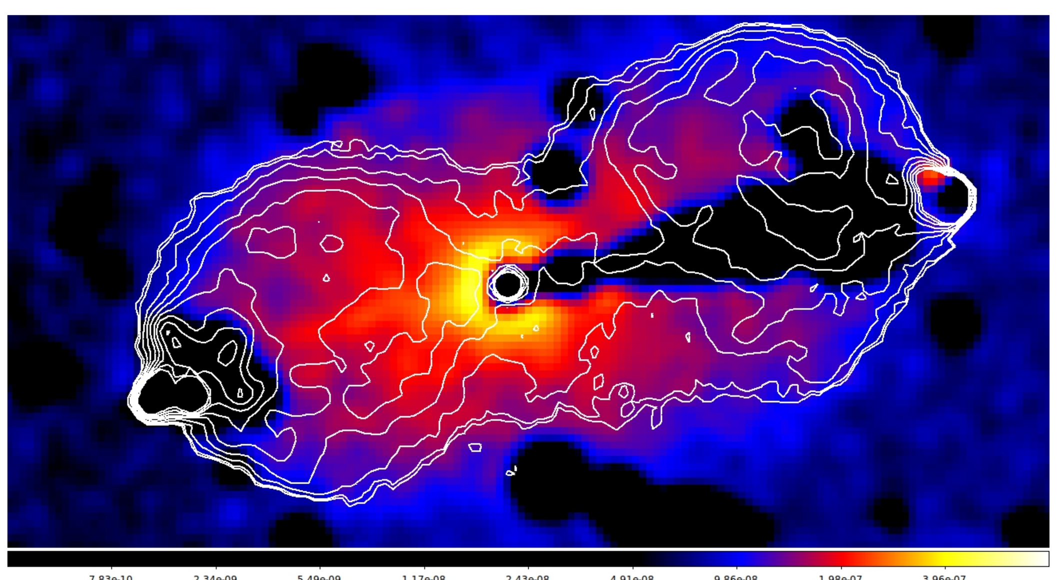

Figure 5: Merged and exposure-corrected smoothed *Chandra* image of the extended lobes in Pictor A in the energy range 0.5–7.0 keV, with the $\lambda 20$ cm, $7.''5$ resolution radio contours superimposed.

VLA $\lambda 20$ cm fractional polarization + *Chandra*

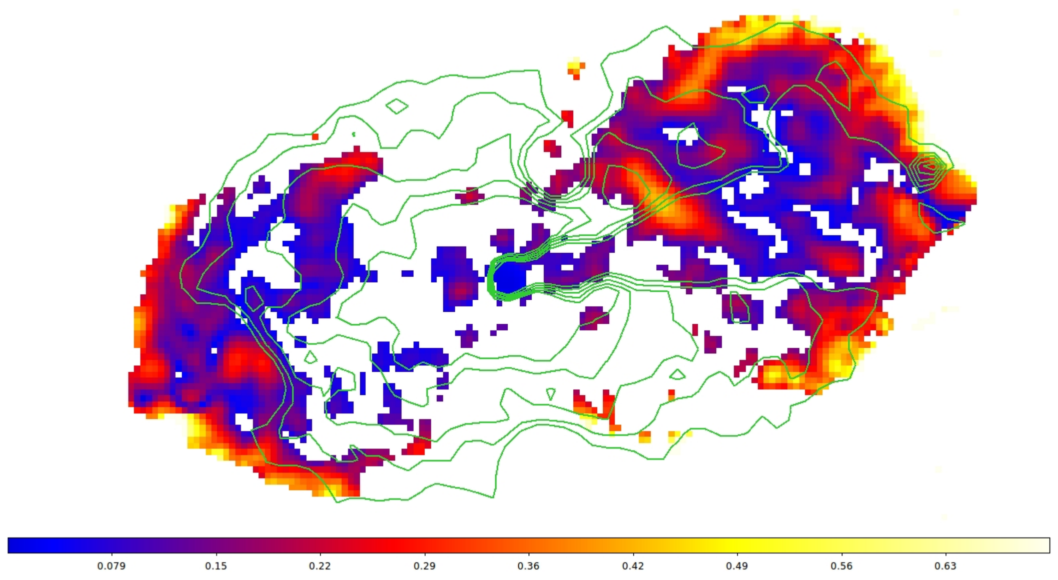

Figure 6: The degree of $\lambda 20$ cm polarization of Pictor A at $10''$ resolution, with the *Chandra* intensity contour superimposed (corresponding to the merged and exposure-corrected image of the extended lobes in the energy range 0.5–7.0 keV).

VLA spectral index + *Chandra*

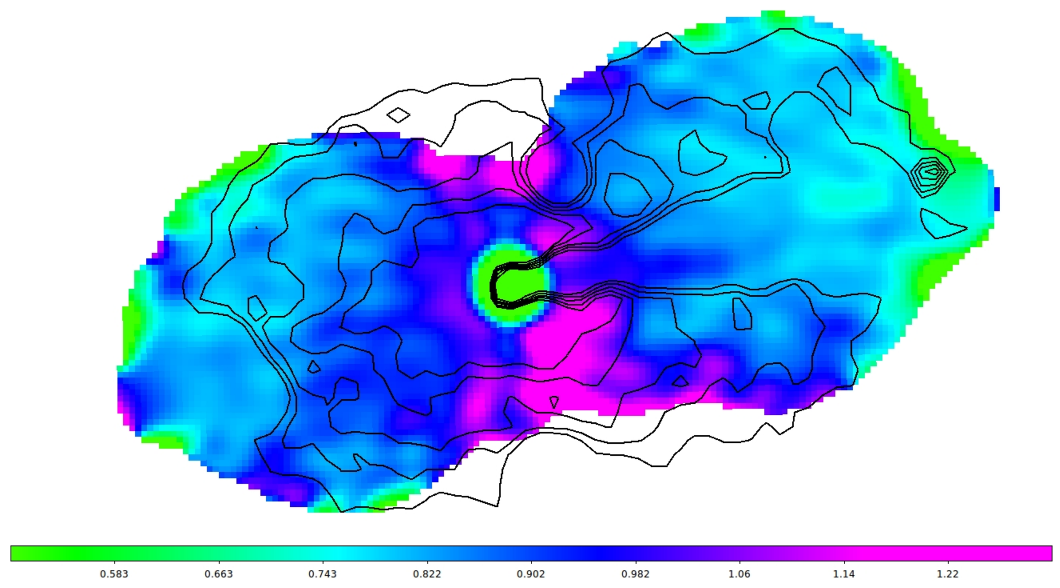

Figure 7: The spectral index ($S_\nu \propto \nu^{-\alpha}$) map between $\lambda 20$ cm and $\lambda 6$ cm at $30''$ resolution, with the *Chandra* intensity contour superimposed (corresponding to the merged and exposure-corrected image of the extended lobes in the energy range 0.5–7.0 keV).

Conclusions & Future work

- The next step of the analysis will include a detailed point-to-point correlation analysis between the X-ray fluxes and radio (total and polarized) fluxes of the extended lobes in Pictor A.
- The preliminary comparison reveal some hints for the correlation between the X-ray intensity and the polarized radio intensity at $\lambda 20$ cm.
- No correlation between the diffuse X-ray flux and radio spectral index (between $\lambda 20$ cm and $\lambda 6$ cm) can be noted.

References

Hardcastle, M. J., Lenc, E., Birkinshaw, M., et al. 2016, MNRAS, 455, 3526
Perley, R. A., Roser, H.-J., & Meisenheimer, K. 1997, A&A, 328, 12

Acknowledgement

This work was supported by the Polish National Science Centre through the grant DEC- 2012/04/A/ST9/00083. A thank R. A. Perley for providing us the radio VLA maps.